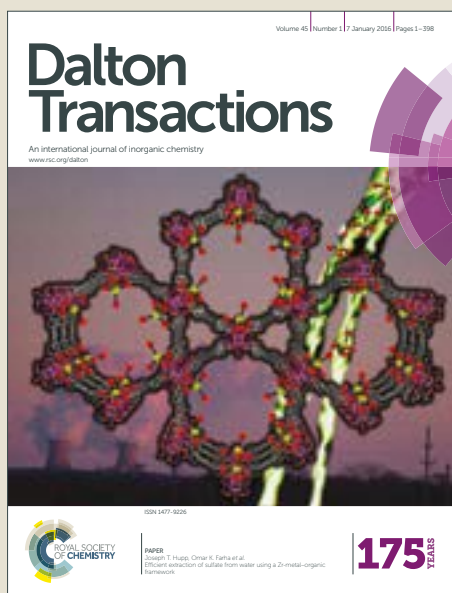


Dalton Transactions

Accepted Manuscript



This article can be cited before page numbers have been issued, to do this please use: S. Konar, A. K. Mondal and M. Sunderarajan, *Dalton Trans.*, 2018, DOI: 10.1039/C7DT04007E.



This is an Accepted Manuscript, which has been through the Royal Society of Chemistry peer review process and has been accepted for publication.

Accepted Manuscripts are published online shortly after acceptance, before technical editing, formatting and proof reading. Using this free service, authors can make their results available to the community, in citable form, before we publish the edited article. We will replace this Accepted Manuscript with the edited and formatted Advance Article as soon as it is available.

You can find more information about Accepted Manuscripts in the [author guidelines](#).

Please note that technical editing may introduce minor changes to the text and/or graphics, which may alter content. The journal's standard [Terms & Conditions](#) and the ethical guidelines, outlined in our [author and reviewer resource centre](#), still apply. In no event shall the Royal Society of Chemistry be held responsible for any errors or omissions in this Accepted Manuscript or any consequences arising from the use of any information it contains.

ARTICLE

A new series of tetrahedral Co(II) complexes [CoLX₂] (X = NCS, Cl, Br, I) manifesting single-ion magnet features

Cite this: DOI: 10.1039/x0xx00000x

Amit Kumar Mondal,^a Mahesh Sundararajan,^{*b} Sanjit Konar^{*a}Received 00th January 2012,
Accepted 00th January 2012

DOI: 10.1039/x0xx00000x

www.rsc.org/

A series of tetrahedral Co^{II} complexes [CoLX₂] (X = NCS (1), Cl (2), Br (3) and I (4); L = 9,9-dimethyl-4,5-bis(diphenylphosphino) xanthene) based on P-donor ligand has been prepared to investigate the influence of terminal ligand field strength on anisotropy of Co^{II} single-ion magnets. It has been observed that heavier and softer terminal ligands are able to decrease the anisotropy of the tetrahedral Co^{II} centers. Thorough analyses of experimental and theoretical studies show that all complexes are having easy-axis type magnetic anisotropy and slow relaxation behaviors of tetrahedral Co^{II} centers. Detailed *ab initio* theory studies disclose that the changes in ligand field strength imposed by the terminal ligands result in modifying the single ion anisotropy (*D*) of complexes 1-4. Furthermore, the isostructural Zn^{II} analogue (5) has been prepared to examine the influence of dipolar interactions between adjacent Co^{II} centres and magnetic dilution experiment was performed.

Introduction

Following the finding of single-molecule magnet (SMM) behavior in the Mn₁₂ complex Mn₁₂O₁₂(CH₃CO₂)₁₆(H₂O)₄,^{1d} several multinuclear 3d metal complexes have been synthesized and their magnetic properties were investigated extensively.^{1,2} In the last few decades, significant efforts have been directed to enhance the effective energy barrier ($U_{\text{eff}} = |D|S^2$) by increasing the ground spin state. Therefore, many polynuclear complexes were reported where strong ferromagnetic coupling between the metal centres were expected to generate high *S* value. Recent studies show that large ground state and high magnetic anisotropy can't be obtained in a single system, therefore multinuclear complexes are probably not the best choices for obtaining higher effective energy barrier. As a consequence

focus has been shifted to single-ion magnets (SIMs) where spin-orbit coupling, which is primarily responsible for magnetic anisotropy, can be reasonably controlled by tuning the strength and geometry of the crystal field. Many mononuclear lanthanide complexes have been reported for showing single ion magnetic behavior^{3,4} and considerable attempts have also been made towards the development of transition metal based SIMs.⁵⁻⁸ Among all reported 3d-SIMs, the most important characteristic is the low coordination environment around metal centre, as by restraining the coordination number magnetic anisotropy can be enhanced in the resulting complex.⁹ In particular, notable attention has been paid on the Co^{II} based SIMs due to its non-integer ground state spin,¹⁰ which actually diminishes the QTM at zero dc field.¹¹ Despite the remarkable developments in the research of SIMs, many essential features of SIMs are still needed to be explored, and hence, further detailed investigation is required.

The reported Co^{II}-SIMs mostly include tricoordinate, tetracoordinate, pentacoordinate, hexacoordinate and heptacoordinate complexes having either positive or negative *D* parameter.⁵⁻⁸ Zero field splitting (ZFS) has been considered by axial parameter, which is associated with energy gap between the ground and excited states. In four coordinated Co^{II} systems, the ground term ⁴A₂(T_d) is split into the ground and excited multiplets and each of them are referring to a Kramers doublet $M_S = \pm 1/2$ and $\pm 3/2$.¹² The efforts to achieve

(a) A. K. Mondal, Dr. S. Konar
Department of Chemistry, Indian Institute of Science Education and Research
Bhopal, Bhopal Bypass road, Bhauri, Bhopal-462066, India. Tel: (+91) 755-
6691313, E-mail: skonar@iiserb.ac.in

(b) Dr. M. Sundararajan
Theoretical Chemistry Section, Bhabha Atomic Research Centre, Mumbai 400085,
India. Tel: (+91) 222-5593829, E-mail: smahesh@barc.gov.in

Electronic Supplementary Information (ESI) available: crystallographic table, coordination polyhedral, SHAPE analysis table, magnetic plots, PXRD, and hydrogen bonding tables are provided CCDC 1460754-1460756. For ESI and crystallographic data in CIF or other electronic format see DOI: 10.1039/x0xx00000x.

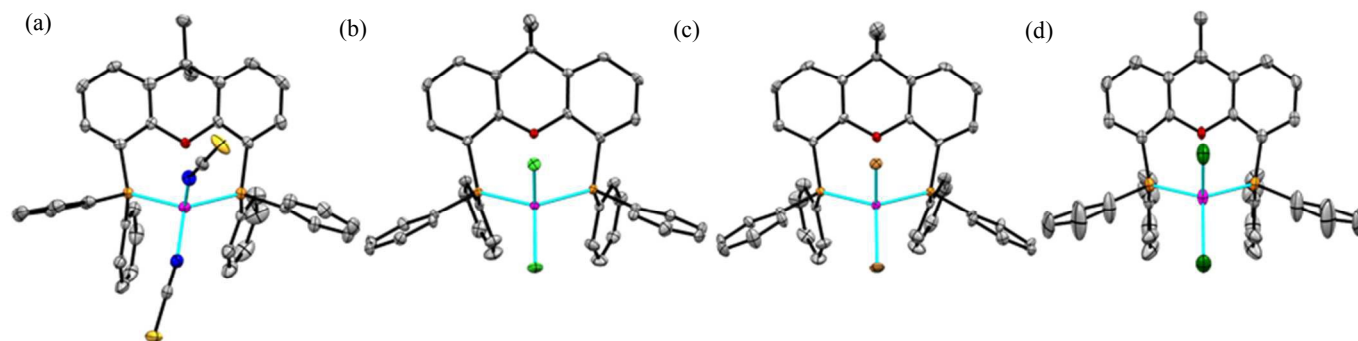
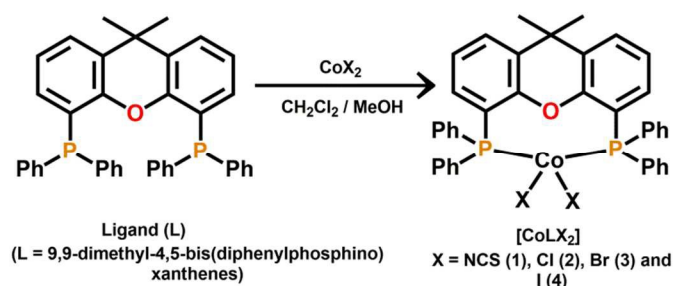


Fig. 1 View of the ellipsoid structures with 50% probability of complexes **1-4** (a-d). Color codes: C (grey), N (blue), O (red), S (yellow), P (orange), Cl (green), Br (brown), I (dark green) and Co (pink).

desired D -parameter in a metal complex by rational synthetic strategy have escalated during recent years and some understandings resulted the magnetostructural D -correlations.¹³ Recently, focus has been given on Co^{II} based tetrahedral system to illustrate the structural dependence of the ZFS parameter.^{12a,14}

For example a series of tetrahedral complexes $[\text{Co}(\text{EPh})_4]^{2-}$ ($\text{E} = \text{O}, \text{S}$ and Se) has been reported by Long *et al.*, where they have shown a substantial increase of the ZFS parameter with heavier donor atoms.^{14e,f} Another series of tetrahedral Co^{II} complexes $[\text{Co}(\text{L})(\text{MeCN})\text{X}_2]$ (where $\text{L} = 2,3$ -diphenyl-1,2,3,4-tetrazolium-5-olate; $\text{X} = \text{Cl}$ or Br) has been also reported to show the similar trend.^{14b} In all cases it has been reported that heavier and softer donor ligands are able to increase the magnetic anisotropy.¹⁵ Similar trend has been found in tetrahedral Co^{II} complexes based on N-donor ligands.^{14c,d} Surprisingly, no such systemic investigation of the influence of heavier and softer donor ligands on the magnetic anisotropy has been made with P-donor ligands. We therefore synthesize a set of tetrahedral Co^{II} complexes based on P-donor ligand to investigate the effect of terminal ligand field strength on anisotropic parameter by combined experimental and theoretical studies. The dynamic magnetization study of tetrahedral Co^{II} complexes $[\text{CoLX}_2]$ ($\text{X} = \text{NCS}$ (**1**), Cl (**2**), Br (**3**) and I (**4**); $\text{L} = 9,9$ -dimethyl-4,5-bis(diphenylphosphino)xanthene) has been investigated and the effect of ligand strength on magnetic anisotropy is also explored.

Results and Discussion



Scheme 1: A reaction scheme illustrating the formation of complexes **1-4**.

Ligand (L) was prepared from 9,9-dimethylxanthene and chlorodiphenylphosphine starting materials and the details synthetic procedure has been given in the experimental section. The tetrahedral Co^{II} complexes $[\text{CoLX}_2]$ ($\text{X} = \text{NCS}$ (**1**), Cl (**2**), Br (**3**) and I (**4**)) were synthesised by reacting the ligand and Co^{II} salts in 1:1 molar ratio (Scheme 1).

Structural Description of Complexes 1-4

Single-crystal X-ray studies of all complexes disclosed that **1** and **4** crystallized in triclinic $P\bar{1}$ and monoclinic $P2_1/m$ space groups respectively, whereas both **2** and **3** crystallized in the monoclinic $P2_1/c$ space groups (Table S1). The Co^{II} centre is coordinated by two phosphorus atoms of the ligand (L) and two terminal ligands X ($\text{X} = \text{NCS}^-$ (**1**), Cl^- (**2**), Br^- (**3**) and I^- (**4**)) (Fig. 1). The local symmetry of the cores $\{\text{CoP}_2\text{X}_2\}$ is almost T_d . The Co-X bond distances increase as ionic radius of terminal atom (X) increases (Table S2) and the angle X-Co-X also increases along the series from **1** to **4**. A clear comparison among the complexes can be made based on their significant structural parameters which have been shown in Table 1. The M-L bond angles in complex **1** are distorted with the angles of $\text{N1-Co-N2} = 114.70(3)$, $\text{N2-Co-P2} = 104.80(4)$ and $\text{P1-Co-P2} = 112.82(4)$ (Table S3). A comparable structure can be found for complex **2** (Fig. 2) with the angles $\text{Cl1-Co-Cl2} = 115.28(3)$, $\text{Cl2-Co-P5} = 108.06(5)$ and $\text{P6-Co-P5} = 114.55(5)$. Complex **3** is isostructural with **2** [$\text{Br1-Co-Br2} = 117.52(2)$, $\text{Br2-Co-P3} = 107.27(2)$ and $\text{P4-Co-P3} = 114.32(1)$] (Table S3). Similar with **3**, complex **4** is having bond angles of $\text{I1-Co-I2} = 118.53(2)$, $\text{I2-Co-P1}' = 105.79(3)$ and $\text{P1-Co-P1}' = 112.92(2)$. The important structural parameters (d , α , β and δ) for complexes **1-4** have been presented in Table 1. The angular

Table 1 Selected structural parameters of complexes **1-4**.

Complex	X	d_L (Å)	d_X (Å)	$\alpha(\text{L-Co-L})$ (°)	$\beta(\text{X-Co-X})$ (°)	δ (°)
1	NCS	2.372	1.924	112.82	114.70	-8.52
2	Cl	2.378	2.221	114.22	116.34	-11.56
3	Br	2.366	2.356	114.67	116.57	-12.24
4	I	2.364	2.554	112.92	118.53	-12.45

d_L = mean distance Co-P , d_X = mean distance Co-X .

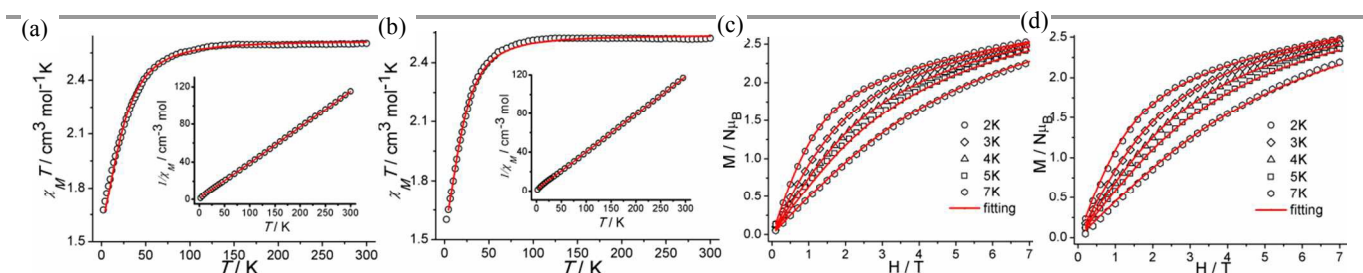


Fig. 2 $\chi_M T$ vs. T plots measured at 0.1 T for complex **1** (a) and **2** (b). $1/\chi_M$ vs. T plots shown in the inset; $M/N\mu_B$ vs. H plots for complexes **1** (c) and **2** (d) at the indicated temperatures. The red lines are the best fit.

distortion parameter δ can be calculated as $\delta = 2 \times T_d - (\alpha + \beta)$ where $\alpha = \text{L-Co-L}$ and $\beta = \text{X-Co-X}$ angles (T_d represents the ideal tetrahedral angle (109.5°)).^{14a} It can be seen that δ show a dependence on nature of the terminal ligand X and it suggests higher distortion from ideal T_d geometry in the series from **1** to **4**. In order to provide more insight into the coordination geometries, SHAPE 2.1¹⁶ analysis has been performed which shows that all Co^{II} centres are having distorted tetrahedral geometries (Fig. S1) with minimum CShM values of 0.281, 0.383, 0.519 and 1.201 for **1-4** respectively. Detailed analyses have been given in the ESI (Table S4).

In complexes **1-4**, substantial π -interaction and intermolecular H-bonding network have been found, that supports formation of supramolecular two dimensional arrangements. In complexes **1-3**, intermolecular H-bonding interactions are formed (Table S5-S7) between the terminal ligands X (X = NCS, Cl and Br) with the phenyl rings and resulted in the construction of 2D arrangements (Fig. S2-S9). The supramolecular 2D arrangement has been also found in complex **4** (Fig. S10-S12) due to strong intermolecular H-bonding interactions between the halogen atoms with solvent molecules (Table S8).

Magnetic Property Studies

Powder X-ray diffraction patterns have been collected for all complexes **1-4** and it indicated the bulk phase purity of all complexes (Fig. S13-S14). Magnetic susceptibility measurements have been performed and the obtained $\chi_M T$ values ($\chi_M =$ molar magnetic susceptibility) were 2.60 (**1**), 2.52 (**2**), 2.47 (**3**) and 2.41 (**4**) $\text{cm}^3 \text{K mol}^{-1}$ at room temperature and the values are found larger than spin-only value of $1.875 \text{ cm}^3 \text{ mol}^{-1} \text{K}$ for Co^{II} ion (Fig. 2 and S15). The obtained $\chi_M T$ values fall within the range for anisotropic Co^{II} centres having

substantial orbital contribution.¹⁷ As the temperature decreases, the $\chi_M T$ values do not change upto 70 K and then it decreases and reaches to the values of 1.48 (**1**), 1.39 (**2**), 1.65 (**3**) and 1.40 (**4**) $\text{cm}^3 \text{ mol}^{-1} \text{K}$ at 2 K (Fig. 2 and S15). Due to inherent anisotropy of the Co^{II} centres, the $\chi_M T$ value decreases at very low temperature. The highest values of magnetization data at 2 K and 7 T were found to be 2.53 (**1**), 2.48 (**2**), 2.43 (**3**) and 2.38 (**4**) $N\mu_B$ (Fig. 2 and S15). The experimental values are observed to be in the lower range than theoretical saturation value of 3.3 (for $g = 2.2$). The magnetization values do not saturate even at 7 T field and the magnetization plots at different temperature do not coincide and that suggests the existence of magnetic anisotropy in studied complexes (Fig. S16). A spin Hamiltonian has been used to quantify the D parameters and that has been described in eqn (1)

$$H = g\mu_B S \cdot B + D[S_z^2 - S(S+1)/3] + E(S_x^2 - S_y^2) \quad (1)$$

the axial and rhombic ZFS parameters have been represented by D and E terms, respectively. D and E parameters were measured using PHI code¹⁸ where $\chi_M T$ vs. T and $M/N\mu_B$ vs. H plots have been fitted simultaneously and the g tensor has been kept isotropic. The best fits gave $D = -16.2(7) \text{ cm}^{-1}$, $E = 1.1(3) \text{ cm}^{-1}$, and $g = 2.27$ for **1**; $D = -15.1(4) \text{ cm}^{-1}$, $E = 0.9(5) \text{ cm}^{-1}$, and $g = 2.24$ for **2**; $D = -11.6(8) \text{ cm}^{-1}$, $E = 1.2(2) \text{ cm}^{-1}$, and $g = 2.20$ for **3**; $D = -7.3(5) \text{ cm}^{-1}$, $E = 1.5(4) \text{ cm}^{-1}$, and $g = 2.18$ for **4**.

The negative D parameters designate the possibility of slow relaxation behaviours for complexes **1-4**. AC magnetic susceptibility measurements have been done at 3.5 Oe ac field in order to check slow magnetic relaxation behaviours. Complexes **1-4** did not display out-of-phase ac signal under

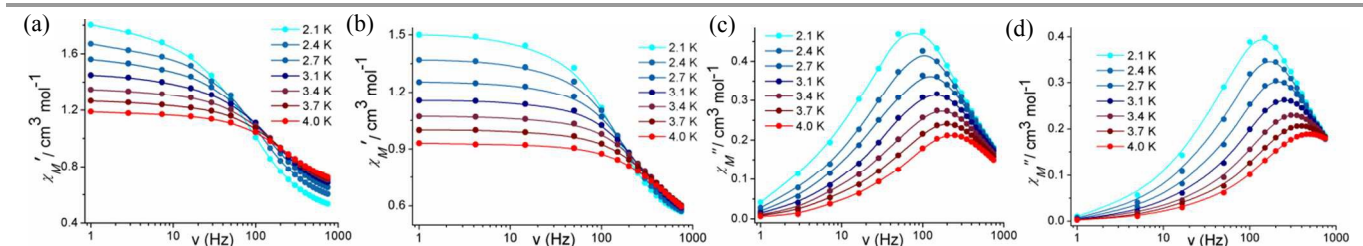


Fig. 3 Frequency dependency of the in-phase (χ_M') (a and b) and out-of-phase (χ_M'') (c and d) AC magnetic susceptibility plots for complex **1** and **2** under 1000 Oe dc field.

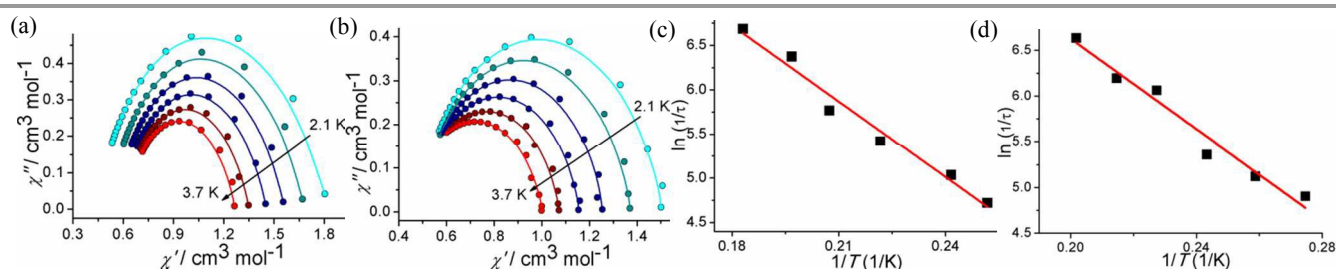


Fig. 4 Cole-Cole plots for complex **1** (a) and **2** (b). Solid lines represent the best fit; $\ln(1/\tau)$ vs. $1/T$ plots for complex **1** (c) and **2** (d). The red lines are the best fit of the Arrhenius relationship.

0 Oe dc field and that might be owing to quantum tunnelling of magnetization (QTM) by thermal relaxation barrier between the $\pm 3/2$ levels. For $S = 3/2$ system with $D < 0$, the QTM process cannot be stimulated by transverse anisotropy through mixing of wave functions corresponding to the $\pm M_s$ levels as a result of the parity effects,¹¹ and therefore, the hyperfine and dipolar arbitrated processes might be responsible for the QTM process.¹⁹ The QTM was suppressed upon application of 1000 Oe dc field which actually splits $\pm M_s$ doublets. Therefore, frequency-dependent ac signals have been found for all complexes and is a characteristic of field-induced 3d-SIMs (Fig. 3 and S17). Moreover, the frequency-dependent ac susceptibility data has been used to make the χ'' vs χ' plots or Cole-Cole plots (Fig. 4 and S18). The modified Debye model²⁰ has been used to fit Cole-Cole plots at different temperature and the α values were obtained (α indicates width of distribution of relaxation times; $\alpha = 1$ and 0 suggests the infinitely wide distributions and relaxation with single time constant, respectively) within the ranges 0.03-0.24 (**1**), 0.06-0.27 (**2**), 0.08-0.30 (**3**) and 0.07-0.32 (**4**) and which indicates narrow distribution of relaxation time. The Arrhenius eqn (2)²¹ was used to measure energy barrier (U_{eff}) and relaxation times (τ_0) for complexes **1-4**

$$\ln(1/\tau) = \ln(1/\tau_0) - U_{\text{eff}}/kT \quad (2)$$

where k is the Boltzmann constant and $1/\tau_0$ is the pre-exponential factor. By using eqn (2), a linear fit has been done and it provided the values of $U_{\text{eff}} = 30.1$ K and $\tau_0 = 6.2 \times 10^{-6}$ s for **1**; $U_{\text{eff}} = 25.5$ K and $\tau_0 = 2.7 \times 10^{-6}$ s for **2**; $U_{\text{eff}} = 18.7$ K and $\tau_0 = 1.8 \times 10^{-6}$ s for **3**; $U_{\text{eff}} = 9.2$ K and $\tau_0 = 1.2 \times 10^{-6}$ s for **4** (Fig. 4 and S18). The obtained τ_0 values are found to be at higher end of SMMs²² and are comparable with the other reported Co^{II} SIMs.^{5f,14e}

The magnetic dilution experiment has been performed to examine the influence of dipolar interactions between adjacent Co^{II} centres. Diamagnetic isostructural Zn^{II} analogue (**5**) was synthesized (Fig. S19 and Table S9) and magnetically diluted with Co^{II} complex (**2**) in a 95:5 percentage ratio. No significant difference in AC measurements for the diluted complex was observed and the obtained energy barriers are found to be almost similar with undiluted complex (Fig. S20). Thus, it can be stated that dipolar interactions are not important in the

present case and slow relaxation occurs from single Co^{II} centres for the studied complexes.

Theoretical Calculations

To get a better understanding of the magnetic anisotropy at the molecular level, detailed theoretical calculations were carried out for all four complexes. DFT optimized structures of the complexes are quite replicated and are consistent with our X-ray data (Fig. S21 and Table S10). The Co-X bond length increases from **1** to **4**, whereas the Co-P bond lengths are almost unaltered. Both P-Co-P (α) and X-Co-X (β) bond angle decreases in the order from **1** to **4**. The electronic structure at the *ab initio* CASSCF-NEVPT2 level was performed to understand the electronic origin of ZFS and to support experimental data. The ZFS on the DFT optimized structures were computed. In fact, computed values for the optimized structures are in better agreement compared to X-ray structure, may perhaps due to packing defects as commonly observed in X-ray structures.

The electronic structures of four Co^{II} complexes were investigated at the *ab initio* level using the newly released ORCA 4.0.1 electronic structure program.^{29b} In Fig. 5, we have plotted five Co^{II} 3d-ligand field splitting orbitals derived from *Ab initio* Ligand Field Theory (AILFT). Unlike the CASSCF derived natural orbitals which are pure, the AILFT orbitals are chemically more meaningful and the mixing with the five 3d-orbitals are taken into account. The one electron orbital energies derived from NEVPT2 wavefunction for all the four species are plotted in Fig. 6. Further, the ligand field splitting parameters of all the four complexes are listed in Table S11.

Although the X-ray crystal structure is close to C_s symmetry, we have not involved any symmetry constraints in our geometry optimizations. However, for the sake of simplistic analysis, we have used C_{2v} symmetry for all four complexes. The ground spin state of all four Co(II) complexes is $S = 3/2$. For the d^7 configuration, the lowest term in spherical symmetry is 4F . Under T_d symmetry, the ground term (4F) splits to 4A_2 , 4T_2 and 4T_1 , whereas the 4A_2 is the lowest in energy and corresponds to $e^4t_2^3$ electronic configuration. Thus, the two e-orbitals, $d_{x^2-y^2}$ and d_{z^2} orbitals are doubly occupied (DOMO), whereas the three t_2 orbitals, d_{xy} , d_{yz} and d_{zx} orbitals are single occupied (SOMO). The splitting between the $d_{x^2-y^2}$ and d_{z^2}

orbital is commonly denoted by μ , whereas the averaged splitting between the t_2 orbitals is denoted by δ . Further, the splitting between the μ and δ is $10Dq$. The computed ligand field splitting parameters for all the four complexes are noted in Table S11.

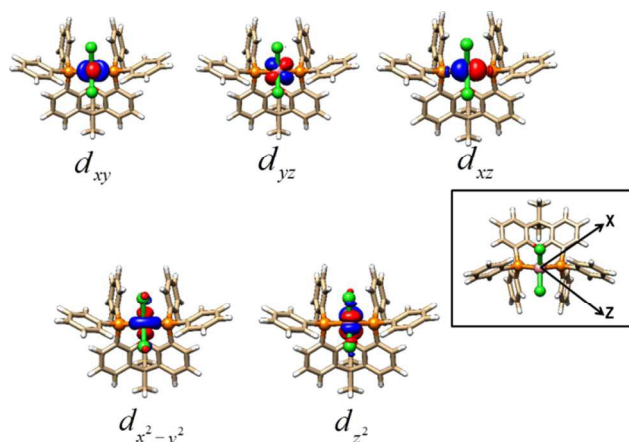


Fig. 5 AILFT derived five 3d-orbitals for complex 2. Inset figure represents the choice of the cartesian axes for complex 2.

In all four complexes, the coordination is varied only by the presence of X group, which can be either isocyanate or three halide anions. Thus, the ligand field strength of the X group is largely responsible for the variable orbital splitting present in these four complexes. Within the four X ligands, the strength of the ligand decreases in the following order, NCS>Cl>Br and I. These variations are reflected in the computed orbital splitting (Fig. 6). The computed $10Dq$, μ and δ decreases from 1 to 4 which reflects the strength of the ligand is largest for NCS and smallest for I. Further, the computed Racah parameters (particularly B) decreases steadily from complex 2 to complex 4 which indicate that Co-X covalency increases from complexes 2 to 4. The AILFT calculated $10Dq$ and the experimental estimates follow the same order. Particularly, in the experimental UV spectrum, we were unable to resolve the chloro and bromo $10Dq$ which estimate to be identical, whereas our computed data clearly indicate that $10Dq$ is smaller for bromo complex (3) thus more softer as compared to chloro complex (2). The computed nephelauxetic parameter, β (cloud expansion) for the four complexes also decreases. The softer I-ligand have a smaller β -value (0.861) is more covalent as compared to stronger Cl-ligand (0.873). Together, our computed LFS is in line with the experimental data.

Let us turn our attention to the computed ZFS parameters which are listed in Table 2. Both the sign and magnitude of D and E values are in excellent agreement with the experimental data for all the four complexes. The computed D_{zz} tensor orientation at the *ab-initio* level have been shown in Fig. S21. In all four complexes, the central Co^{II} is at origin, whereas X is orientated in Z-axis and thus the computed D_{zz} is along the Co-X bond. Further, as the spin-spin contributions to ZFS is very small, the computed D -value arises from spin-orbit coupling (SOC) with the excited state, particularly the spin allowed first excited

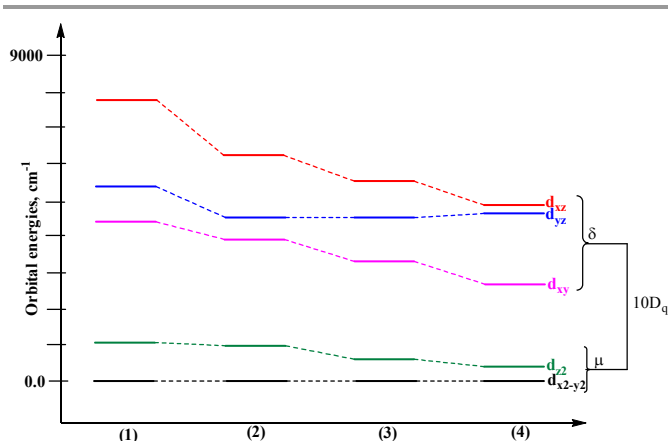


Fig. 6 A comparison of NEVPT2 AILFT orbital energies for the four complexes studied here. μ and δ denotes averaged e and t_2 energies and $10Dq$ denotes the energy difference between μ and δ .

state.^{9e,12a,14g-h,15a} These spin-allowed transitions are commonly denoted as ${}^4A_2 \rightarrow {}^4T_2(\text{F})$ (denoted as Δ_1). Similarly, other transitions are denoted as ${}^4A_2 \rightarrow {}^4T_1(\text{F})$, denoted as Δ_2 and ${}^4A_2 \rightarrow {}^4T_1(\text{P})$ (denoted as Δ_3) which sums up to 9 transitions corresponding to the quartet state (Table S12). In general CASSCF transition energies show large errors as compared to the experimental data, whereas transition energies corrected for dynamic correlation derived from NEVPT2 calculations are more accurate (Table S12) For all the four complexes, the Δ_1 transitions are typically less than $10,000 \text{ cm}^{-1}$. It should be noted that the computed transition energy error bars can vary from 2000 to 4000 cm^{-1} when compared with experiments.

Table 2 Computed values D and E and their dominant contributions arising from quartet and doublet states.^a

	1	2	3	4
D	-15.9 (-16.2)	-15.5 (-15.1)	-12.7 (-11.6)	-9.6 (-7.3)
E	1.1 (1.1)	0.5 (0.9)	0.6 (1.2)	1.3 (1.5)
${}^4T_2(\text{F})$	-28.6	-28.7	10.2	11.5
${}^4T_2(\text{F})$	7.4	9.0	-27.4	-21.7
${}^4T_2(\text{F})$	7.3	8.9	9.2	9.9
${}^4T_1(\text{F})$	-0.4	-3.5	-4.4	-5.3
${}^2E(\text{G})$	-1.2	-1.2	-1.0	-0.9
${}^2T_2(\text{G})$	3.8	3.5	3.8	-2.6
${}^2T_2(\text{G})$	-3.3	-2.8	-2.5	3.9
${}^2T_2(\text{G})$	-2.7	-2.5	-2.4	-2.4

^a Experimental values in brackets

Within the four complexes and in all three transitions (Δ_1 to Δ_3), the splitting is largest for 1 (X = NCS) and smallest for 4 (X = I) which qualitatively follows the strength of ligand field in decreasing order from NCS to I and also follow ZFS order (Table 3). However, the doublet term arising from 2G also

contribute the transitions which are spin forbidden. As far as the individual contributions to ZFS are concerned, we find that low lying 4T_2 (F) dictate the sign and the magnitude of ZFS (more than 80%). For complex **1**, Δ_1 contribution is larger than other quartet terms such as Δ_2 and Δ_3 , whereas the contribution of Δ_2 becoming more important for the other halo complexes, particularly for the iodo complex. Similarly, the doublet term contribution (2T_2 arising from 2G) is again less which cancel out each other. For instance, in **4**, the values are -2.6, -2.4 and +3.9, thus their overall contribution to D is negligible.

Table 3 Computed d-d transitions (in cm^{-1}) at the NEVPT2 level for complexes **1-4**.

	1	2	3	4
$^4A_2 \rightarrow ^4T_2(\text{F})$	5092.1	4248.4	4094.7	3834.1
$^4A_2 \rightarrow ^4T_2(\text{F})$	5445.5	4450.6	4220.5	4298.3
$^4A_2 \rightarrow ^4T_2(\text{F})$	7567.2	6140.8	5862.2	5563.5
$^4A_2 \rightarrow ^4T_1(\text{F})$	8221.6	7385	7258.7	7242
$^4A_2 \rightarrow ^4T_1(\text{F})$	10011.2	8744.2	8428.8	8254.6
$^4A_2 \rightarrow ^4T_1(\text{F})$	13232.7	11941.4	11526.5	11172.5
$^4A_2 \rightarrow ^4T_1(\text{P})$	17971.2	17934.2	18306.6	18829.9
$^4A_2 \rightarrow ^4T_1(\text{P})$	22159.3	21057.3	20611.1	20221.3
$^4A_2 \rightarrow ^4T_1(\text{P})$	23849.2	21959	21071	20281.8

The difference in the predicted ZFS for the four complexes discussed above can arise due to several factors, which are discussed below.

Variable oxygen interaction with Co(II) centre:

In all the four complexes discussed above, there exist variable but weak Co-O distance (2.887 Å for complex **3** to 3.246 Å for **1**) which could influence the predicted ZFS. We have performed constrained (Co-O = 2.887 Å and 3.246 Å) geometry optimization of the Co-chloro structure and computed the ZFS at the NEVPT2 level. For Co-O = 2.887 Å ($D = -15.5 \text{ cm}^{-1}$) and Co-O = 3.246 Å ($D = -15.9 \text{ cm}^{-1}$) species, the predicted ZFS differ by less than 0.5 cm^{-1} . Thus, the effect of oxygen interaction with Co(II) is rather minimal.

Variation of first coordination ligands:

In the studies of Long and co-workers^{14f} and in Neese and co-workers^{14j} on CoX_4 ligands (where X = OPh, SPh, SePh), the estimated and computed ZFS increases from oxygen (-11 cm^{-1}) to sulfur (-62 cm^{-1}) to selenium (-83 cm^{-1}) which was claimed as heavy atom effect. The origin of the increased ZFS is largely due to the increased contribution of arising from lowest 4T_2

state (due to SOC) from oxygen to sulfur to selenium. However, we found here that increasing the halide ions from chloro to bromo to iodo, the computed (or estimated) ZFS decreases from complexes **2** to **4**. Our predicted trends in the ZFS is consistent with those of Smolko *et al* for a series of tetra-coordinate Co(II) complexes $\{\text{Co}(\text{biq})\text{X}_2\}$ (where biq = biquinoline ligand and X = Cl, Br and I).^{14c} For these complexes, the predicted ZFS again decreases which is in line with our observations. A similar trend is also found for $\text{CoCl}_2(\text{PPh}_3)_2$ ($D = -14.76 \text{ cm}^{-1}$) and $\text{CoBr}_2(\text{PPh}_3)_2$ ($D = -13.90 \text{ cm}^{-1}$) complexes by Lu *et al*.^{14k} To what extent the geometric distortions upon halide substitution alter the ZFS are also investigated. Replacing the Cl ligand by Br (Co-Br = 2.330 Å) and I (Co-I = 2.550 Å) in complex **2**, the computed ZFS alter by less than 1 cm^{-1} when compared to the corresponding ZFS of complexes **3** and **4**. These variations in ZFS clearly suggest halide ion effect is dominant as compared to geometric distortions. Thus, we can claim that halide ion clearly plays a dominant role which can modify the ZFS and we can coin the term it as halide ion effect.

Dunbar and co-workers^{14a} reported the ZFS for a series of CoA_2B_2 complexes with differing A (A = N, P and As) and B (B = Cl, Br and I). Unlike our work predictions, they found that ZFS increases from Cl ($D = -11.6 \text{ cm}^{-1}$) to Br ($D = -12.5 \text{ cm}^{-1}$) to I ($D = -36.9 \text{ cm}^{-1}$). Similarly the ZFS again increases from CoN_2I_2 ($D = +9.2 \text{ cm}^{-1}$), CoP_2I_2 ($D = -36.9 \text{ cm}^{-1}$) and CoAs_2I_2 ($D = -74.7 \text{ cm}^{-1}$). To estimate the effect of π -acceptor P vs As, we have computed the ZFS of As analogs of **2** and **4**. Our computed ZFS for the As analog are -37.5 cm^{-1} (CoAs_2Cl_2) and -17.5 cm^{-1} (CoAs_2I_2) which is against the predictions of Dunbar and co-workers.^{14a}

Conclusions

A series of Co^{II} based tetrahedral complexes have been synthesized and quantitative estimation of magnetic anisotropy using detailed *ab initio* theory studies disclose that the differences in ligand field strength imposed by the terminal ligands result in modifying the single ion anisotropy (D) at the metal centre. The present results also demonstrate the presence of field induced slow relaxation behaviors in a series of tetrahedral Co^{II} complexes. It has been revealed that heavier and softer terminal ligands can decrease the anisotropy of tetrahedral Co^{II} centres; and thus attaining a quantitative magnetostructural correlation.

Experimental Section

Materials and Methods

Magnetic measurements were performed using a Quantum Design SQUID-VSM magnetometer. The measured values were corrected for the experimentally measured contribution of the sample holder, while the derived susceptibilities were corrected for the diamagnetic contribution of the sample, estimated from Pascal's tables.²³ Elemental analysis was performed on Elementar Microvario Cube Elemental Analyzer.

IR spectrum was recorded on KBr pellets with a Perkin-Elmer spectrometer. Powder X-ray diffraction (PXRD) data was collected on a PANalytical EMPYREAN instrument using Cu-K α radiation.

X-ray Crystallography

Intensity data were collected on a Bruker APEX-II CCD diffractometer using a graphite monochromated Mo-K α radiation ($\alpha = 0.71073 \text{ \AA}$). Data collection was performed using ϕ and ω scan. The structure was solved using direct methods followed by full matrix least square refinements against F^2 (all data HKLF 4 format) using SHELXTL.²⁴ Subsequent difference Fourier synthesis and least-square refinement revealed the positions of the remaining non-hydrogen atoms. Determinations of the crystal system, orientation matrix, and cell dimensions were performed according to the established procedures. Lorentz polarization and multi-scan absorption correction was applied. Non-hydrogen atoms were refined with independent anisotropic displacement parameters and hydrogen atoms were placed geometrically and refined using the riding model. All calculations were carried out using SHELXL 97,²⁵ PLATON 99,²⁶ and WinGX system Ver-1.64.²⁷ Crystallographic data for complexes 1-5 were summarized in Table S1.

Computational Details

The four X-ray structures are optimized at the DFT level using BP86 functional and TZVP basis set. All structures are verified as minima through the computation of vibrational frequencies. We have used this computational strategy for a number of transition metal systems where good geometric predictions are made.²⁸ Ab initio calculations are performed using CASSCF multi-configurational method for the computation of zero field splitting and d-d transitions. To recover the dynamic correlation, NEVPT2 calculations are carried out on top of the CASSCF wave function. In all four complexes, we have used 7 electrons in 5 d-orbitals in the active space. All calculations are performed using ORCA 3.0.3^{29a} and 4.0.1.^{29b} In the ab initio calculations, a def2-TZVPP basis set is used for Co, P, S, O, C, Cl, Br, I are treated with def2-TZVP basis set, whereas the C and H are described using def2-SV(P) basis set. For the complex 4, an all electron Sapporo-DKH3-TZP-2012 basis set is used.^{29c} Both geometry optimizations and ZFS calculations are carried out with scalar relativistic effects using ZORA (except complex 4). Spin-orbit coupling calculations are carried out within Quasi-degenerate Perturbation Theory (QDPT) as implemented by Ganyushin and Neese.³⁰ For Co^{II} complexes, the SOC contribution is very large, whereas the spin-spin coupling contribution to ZFS is negligible (less than 2%), thus not included in our calculations.

Synthesis

Synthesis of ligand

9,9-dimethylxanthene (1.00 g, 4.76 mmol) was added to 60 ml of dry Et₂O solution of TMEDA (2.1 ml, 13.3 mmol) and the solution was stirred for 1 hr. Then, *sec*-butyllithium (12.5 ml,

13.3 mmol) was added to the previous mixture while stirring at room temperature. The whole reaction mixture was stirred for additional 15 hrs. Then 16 ml hexanes solution of chlorodiphenylphosphine (2.6 ml, 13.3 mmol) was added and stirred for additional 15 hrs. The solvent was removed and the solid was dissolved in CH₂Cl₂; and then washed with H₂O. The solvent was removed and the obtained final product was washed with hexanes and crystallized from 1-propanol to give 2.02 g (74 %) of yellow-white powder. ¹H NMR (CDCl₃): δ 7.40 (dd), 7.18 (m), 6.96 (t), 6.54 (dd), 1.65 (s). Selected IR data (KBr pellet, 4000 – 400 cm⁻¹) ν /cm⁻¹: 3075 (ν_{C-H}), 2973 (ν_{C-H}), 1404 (ν_{Ar-H}), 746 (ν_{C-CH}), 694 (ν_{C-CH}).

Synthesis of complex 1

Ligand (57 mg, 0.1 mmol) was dissolved in 5 ml of CH₂Cl₂ then 5 ml methanolic solution of Co(NCS)₂ (18 mg, 0.1 mmol) was added dropwisely to above solution. The whole reaction mixture forms blue color and solution was stirred for additional 2 hrs. The mixture was filtered and filtrate was kept for slow evaporation that gives blue crystals of Co(L)(NCS)₂ (1) after 3 days. The crystals were washed with H₂O and Et₂O and air-dried yield (83 %). Anal. Calcd for C₄₁H₃₂CoN₂O₂S₂: C, 65.33; H, 4.28; N, 3.72; S, 8.49 %. Found: C, 65.46; H, 4.37; N, 3.78; S, 8.56 %. Selected IR data (KBr pellet, 4000 – 400 cm⁻¹) ν /cm⁻¹: 3062 (ν_{C-H}), 2976 (ν_{C-H}), 2034 (ν_{NCS}), 1410 (ν_{Ar-H}), 741 (ν_{C-CH}), 698 (ν_{C-CH}).

Following the similar synthetic method, complexes 2-4 were synthesized using CoCl₂, CoBr₂ and CoI₂ respectively.

Synthesis of complex 2

Yield 78%. Elemental analysis; Anal. Calcd for C₃₉H₃₂Cl₂CoOP₂: C, 66.10; H, 4.55 %. Found: C, 66.21; H, 4.63 %. Selected IR data (KBr pellet, 4000 – 400 cm⁻¹) ν /cm⁻¹: 3057 (ν_{C-H}), 2972 (ν_{C-H}), 1412 (ν_{Ar-H}), 738 (ν_{C-CH}), 697 (ν_{C-CH}).

Synthesis of complex 3

Yield 70%. Elemental analysis; Anal. Calcd for C₃₉H₃₂Br₂CoOP₂: C, 58.73; H, 4.05 %. Found: C, 58.85; H, 3.98 %. Selected IR data (KBr pellet, 4000 – 400 cm⁻¹) ν /cm⁻¹: 3060 (ν_{C-H}), 2975 (ν_{C-H}), 1415 (ν_{Ar-H}), 743 (ν_{C-CH}), 696 (ν_{C-CH}).

Synthesis of complex 4

Yield 72%. Elemental analysis; Anal. Calcd for C₄₂H₄₀Cl₂I₂CoO₅P₂: C, 47.11; H, 3.77 %. Found: C, 47.22; H, 3.87 %. Selected IR data (KBr pellet, 4000 – 400 cm⁻¹) ν /cm⁻¹: 3056 (ν_{C-H}), 2972 (ν_{C-H}), 1411 (ν_{Ar-H}), 740 (ν_{C-CH}), 693 (ν_{C-CH}).

Acknowledgements

A.K.M. thanks UGC, India for the SRF fellowship. S.K. thanks BRNS DAE (Project 37(2)/14/09/2015-BRNS) and IISER Bhopal for generous financial support. A.K.M. thanks Mr. Vijay Singh Parmar and Dr. Subhadip Roy for helpful scientific discussion. M.S. thanks Mr. Arup Sarkar and Dr. Gopalan Rajaraman of IIT-Bombay for their helpful discussion.

ARTICLE

Notes and references

† Electronic Supplementary Information (ESI) available: crystallographic table, coordination polyhedral, SHAPE analysis table, magnetic plots, PXRD, and hydrogen bonding tables are provided. CCDC 1460754-1460756. See DOI: 10.1039/b000000x.

§
§§
etc.

- (a) A. Caneschi, D. Gatteschi, R. Sessoli, A. L. Barra, L. C. Brunel and M. Guillot, *J. Am. Chem. Soc.*, 1991, **113**, 5873; (b) R. Sessoli, D. Gatteschi, A. Caneschi and M. A. Novak, *Nature*, 1993, **365**, 141; (c) C. Delfs, D. Gatteschi, L. Pardi, R. Sessoli, K. Wieghardt and D. Hanke, *Inorg. Chem.*, 1993, **32**, 3099; (d) R. Sessoli, H. L. Tsai, A. R. Schake, S. Y. Wang, J. B. Vincent, K. Folting, D. Gatteschi, G. Christou and D. N. Hendrickson, *J. Am. Chem. Soc.*, 1993, **115**, 1804; (e) D. Gatteschi, A. Caneschi, L. Pardi and R. Sessoli, *Science*, 1994, **265**, 1054; (f) A. L. Barra, A. Caneschi, A. Cornia, F. F. de Biani, D. Gatteschi, C. Sangregorio, R. Sessoli and L. Sorace, *J. Am. Chem. Soc.*, 1999, **121**, 5302; (g) E. K. Brechin, J. Yoo, M. Nakano, J. C. Huffman, D. N. Hendrickson and G. Christou, *Chem. Commun.*, 1999, 783; (h) S. Maheswaran, G. Chastanet, S. J. Teat, T. Mallah, R. Sessoli, W. Wernsdorfer and R. E. P. Winpenny, *Angew. Chem., Int. Ed.*, 2005, **44**, 5044.
- (a) M. N. Leuenberger and D. Loss, *Nature*, 2001, **410**, 789; (b) L. Bogani and W. Wernsdorfer, *Nat. Mater.*, 2008, **7**, 179.
- N. Ishikawa, M. Sugita, T. Ishikawa, S.-Y. Koshihara and Y. Kaizu, *J. Am. Chem. Soc.*, 2003, **125**, 8694.
- (a) R. J. Blagg, C. A. Murny, E. J. L. McInnes, F. Tuna and R. E. P. Winpenny, *Angew. Chem., Int. Ed.*, 2011, **50**, 6530; (b) J. D. Rinehart, M. Fang, W. J. Evans and J. R. Long, *Nat. Chem.*, 2011, **3**, 538; (c) J. D. Rinehart, M. Fang, W. J. Evans and J. R. Long, *J. Am. Chem. Soc.*, 2011, **133**, 14236; (d) J. J. Le Roy, L. Ungur, I. Korobkov, L. F. Chibotaru and M. Murugesu, *J. Am. Chem. Soc.*, 2014, **136**, 8003; (e) L. Ungur, J. J. Le Roy, I. Korobkov, M. Murugesu and L. F. Chibotaru, *Angew. Chem., Int. Ed.*, 2014, **53**, 4413; (f) L. J. Batchelor, I. Cimatti, R. Guillot, F. Tuna, W. Wernsdorfer, L. Ungur, L. F. Chibotaru, V. E. Campbell and T. Mallah, *Dalton Trans.*, 2014, **43**, 12146; (g) V. E. Campbell, H. Bolvin, E. Rivière, R. Guillot, W. Wernsdorfer and T. Mallah, *Inorg. Chem.*, 2014, **53**, 2598; (h) S.-D. Jiang, B.-W. Wang, H.-L. Sun, Z.-M. Wang and S. Gao, *J. Am. Chem. Soc.*, 2011, **133**, 4730; (i) A. K. Mondal, S. Goswami and S. Konar, *Dalton Trans.*, 2015, **44**, 5086; (j) D. N. Woodruff, R. E. P. Winpenny and R. A. Layfield, *Chem. Rev.*, 2013, **113**, 5110; (k) J. D. Rinehart and J. R. Long, *Chem. Sci.*, 2011, **2**, 2078; (l) F. Habib and M. Murugesu, *Chem. Soc. Rev.*, 2013, **42**, 3278; (m) P. Zhang, Y. N. Guo and J. Tang, *Coord. Chem. Rev.*, 2013, **257**, 1728; (n) S. Goswami, A. K. Mondal and S. Konar, *Inorg. Chem. Front.*, 2015, **2**, 687; (o) S. K. Gupta, T. Rajeshkumar, G. Rajaraman and R. Murugavel, *Chem. Sci.*, 2016, **7**, 5181; (p) A. J. Brown, D. Pinkowicz, M. R. Saber and K. R. Dunbar, *Angew. Chem. Int. Ed.*, 2015, **54**, 5864; (q) J. Liu, Y.-C. Chen, J.-L. Liu, V. Vieru, L. Ungur, J.-H. Jia, L. F. Chibotaru, Y. Lan, W. Wernsdorfer, S. Gao, X.-M. Chen and M.-L. Tong, *J. Am. Chem. Soc.*, 2016, **138**, 5441; (r) Y.-C. Chen, J.-L. Liu, L. Ungur, J. Liu, Q.-W. Li, L.-F. Wang, Z.-P. Ni, L. F. Chibotaru, X.-M. Chen and M.-L. Tong, *J. Am. Chem. Soc.*, 2016, **138**, 2829; (s) Y.-S. Meng, S.-D. Jiang, B.-W. Wang and S. Gao, *Acc. Chem. Res.*, 2016, **49**, 2381.
- (a) W. H. Harman, T. D. Harris, D. E. Freedman, H. Fong, A. Chang, J. D. Rinehart, A. Ozarowski, M. T. Sougrati, F. Grandjean, G. J. Long, J. R. Long and C. J. Chang, *J. Am. Chem. Soc.*, 2010, **132**, 18115; (b) D. Weismann, Y. Sun, Y. Lan, G. Wolmershäuser, A. K. Powell and H. Sitzmann, *Chem. - Eur. J.*, 2011, **17**, 4700; (c) P. H. Lin, N. C. Smythe, S. I. Gorelsky, S. Maguire, N. J. Henson, I. Korobkov, B. L. Scott, J. C. Gordon, R. T. Baker and M. Murugesu, *J. Am. Chem. Soc.*, 2011, **133**, 15806; (d) S. Mossin, B. L. Tran, D. Adhikari, M. Pink, F. M. Heinemann, J. Sutter, R. K. Szilagy, K. Meyer and D. J. Mindiola, *J. Am. Chem. Soc.*, 2012, **134**, 13651; (e) J. M. Zadrozny, M. Atanasov, A. M. Bryan, C. Y. Lin, B. D. Recken, P. P. Power, F. Neese and J. R. Long, *Chem. Sci.*, 2013, **4**, 125; (f) T. Jurca, A. Farghal, P. H. Lin, I. Korobkov, M. Murugesu and D. S. Richardson, *J. Am. Chem. Soc.*, 2011, **133**, 15814; (g) J. M. Zadrozny, J. Liu, N. A. Piro, C. J. Chang, S. Hill and J. R. Long, *Chem. Commun.*, 2012, **48**, 3927; (h) J. Vallejo, I. Castro, R. R. García, J. Cano, M. Julve, F. Lloret, G. D. Munno, W. Wernsdorfer and E. Pardo, *J. Am. Chem. Soc.*, 2012, **134**, 15704; (i) G. A. Craig and M. Murrie, *Chem. Soc. Rev.*, 2015, **44**, 2135; (j) R. Ruamps, R. Maurice, L. Batchelor, M. Boggio-Pasqua, R. Guillot, A. L. Barra, J. J. Liu, E. Bendeif, S. Pillet, S. Hill, T. Mallah and N. Guihery, *J. Am. Chem. Soc.*, 2013, **135**, 3017; (k) S. Gómez-Coca, E. Cremades, N. Aliaga-Alcalde and E. Ruiz, *Inorg. Chem.*, 2014, **53**, 676; (l) S. Gómez-Coca, D. Aravena, R. Morales and E. Ruiz, *Coord. Chem. Rev.*, 2015, **289**, 379; (m) A. K. Bar, C. Pichon and J. Sutter, *Coord. Chem. Rev.*, 2016, **308**, 346; (n) A. K. Mondal, S. Khatua, K. Tomar and S. Konar, *Eur. J. Inorg. Chem.*, 2016, 3545.
- (a) P. P. Samuel, K. C. Mondal, N. A. Sk, H. W. Roesky, E. Carl, R. Neufeld, D. Stalke, S. Demeshko, F. Meyer, L. Ungur, L. F. Chibotaru, J. Christian, V. Ramachandran, J. Tol and N. S. Dalal, *J. Am. Chem. Soc.*, 2014, **136**, 11964; (b) A. K. Mondal, J. Jover, E. Ruiz and S. Konar, *Chem. Commun.*, 2017, **53**, 5338; (c) A. K. Mondal, T. Goswami, A. Misra and S. Konar, *Inorg. Chem.*, 2017, **56**, 6870.
- (a) C. Mathonière, H.-J. Lin, D. Siretanu, R. Clérac and J. M. Smith, *J. Am. Chem. Soc.*, 2013, **135**, 19083; (b) A. K. Mondal, J. Jover, E. Ruiz and S. Konar, *Chem. Eur. J.*, 2017, **23**, 12550; (c) X. Feng, C. Mathonière, I.-R. Jeon, M. Rouzières, A. Ozarowski, M. L. Aubrey, M. I. Gonzalez, R. Clérac and J. R. Long, *J. Am. Chem. Soc.*, 2013, **135**, 15880.
- (a) Y. Y. Zhu, C. Cui, Y. Q. Zhang, J. H. Jia, X. Guo, C. Gao, K. Qian, S. D. Jiang, B. W. Wang, Z. M. Wang and S. Gao, *Chem. Sci.*, 2013, **4**, 1802; (b) S. Gómez-Coca, E. Cremades, N. Aliaga-Alcalde and E. Ruiz, *J. Am. Chem. Soc.*, 2013, **135**, 7010; (c) F. Yang, Q. Zhou, Y. Zhang, G. Zeng, G. Li, Z. Shi, B. Wang and S. Feng, *Chem. Commun.*, 2013, **49**, 5289; (d) D. Wu, X. Zhang, P. Huang, W. Huang, M. Ruan and Z. W. Ouyang, *Inorg. Chem.*, 2013, **52**, 10976; (e) W. Huang, T. Liu, D. Wu, J. Cheng, Z. W. Ouyang and C. Duan, *Dalton Trans.*, 2013, **42**, 15326; (f) R. Herchel, L. Váhovská, I. Potočník and Z. Trávníček, *Inorg. Chem.*, 2014, **53**, 5896; (g) A. K. Mondal, V. S. Parmar, S. Biswas and S. Konar, *Dalton Trans.*, 2016, **45**, 4548; (h) Y. Rechkemmer, F. D. Breitgoff, M. van der Meer, M. Atanasov, M. Hakl, M. Orlita, P. Neugebauer, F. Neese, B. Sarkar and J. van Slageren, *Nat. Commun.*, 2016, **7**, 10467; (i) D. Schweinfurth, J. Krzystek, M. Atanasov, J. Klein, S. Hohloch, J. Telsler, S. Demeshko, F. Meyer, F. Neese and B. Sarkar, *Inorg. Chem.*, 2017, **56**, 5253.
- (a) J. M. Zadrozny, D. J. Xiao, M. Atanasov, G. J. Long, F. Grandjean, F. Neese and J. R. Long, *Nat. Chem.*, 2013, **5**, 577; (b) R. C. Poulton, M. J. Page, A. G. Algarra, J. J. Le Roy, I. Lopez, E. Carter, A. Llobet, S. A. Macgregor, M. F. Mahon, D. M. Murphy, M. Murugesu and M. K. Whittlesey, *J. Am. Chem. Soc.*, 2013, **135**, 13640; (c) Y.-Z. Zhang, S. Gómez-Coca, A. J. Brown, M. R. Saber, X. Zhang and K. R. Dunbar, *Chem. Sci.*, 2016, **7**, 6519; (d) R. Boča, J. Miklovič and J. Titiš, *Inorg. Chem.*, 2014, **53**, 2367; (e) D. Brazzolotto, M. Gennari, S. Yu, J. Pécaut, M. Rouzières, R. Clérac, M. Orío and C. Duboc, *Chem. Eur. J.*, 2016, **22**, 925; (f) X.-N. Yao, J.-Z. Du, Y.-Q. Zhang, X.-B. Leng, M.-W. Yang, S.-D. Jiang, Z.-X. Wang, Z.-W. Ouyang, L. Deng, B.-W. Wang and S. Gao, *J. Am. Chem. Soc.*, 2017, **139**, 373; (g) T. J. Woods, M. F. Ballesteros-Rivas, S. Gómez-Coca, E. Ruiz and K. R. Dunbar, *J. Am. Chem. Soc.*, 2016, **138**, 16407.
- (a) A. Caneschi, D. Gatteschi, N. Lalioi, C. Sangregorio, R. Sessoli, G. Venturi, A. Vindigni, A. Rettori, M. G. Pini and M. A. Novak, *Angew. Chem., Int. Ed.*, 2001, **40**, 1760; (b) M. Murrie, *Chem. Soc. Rev.*, 2010, **39**, 1986.
- H. A. Kramers, *Proc. R. Acad. Sci. Amsterdam*, 1930, **33**, 959.
- (a) M. Idešicová, J. Titiš, J. Krzystek and R. Boča, *Inorg. Chem.*, 2013, **52**, 9409; (b) D. Maganas, S. Sottini, P. Kyritsis, E. J. J. Groenen and F. Neese, *Inorg. Chem.*, 2011, **50**, 8741.
- (a) J. Titiš and R. Boča, *Inorg. Chem.*, 2010, **49**, 3971; (b) I. Nemeč, R. Herchel, I. Svoboda, R. Boča and Z. Trávníček, *Dalton Trans.*,

- 2015, **44**, 9551; (c) S. K. Singh, T. Gupta, P. Badkur and G. Rajaraman, *Chem. Eur. J.*, 2014, **20**, 10305; (d) J. Titiš and R. Boča, *Inorg. Chem.*, 2011, **50**, 11838.
14. (a) M. R. Saber and K. R. Dunbar, *Chem. Commun.*, 2014, **50**, 12266; (b) S. Vaidya, A. Upadhyay, S. K. Singh, T. Gupta, S. Tewary, S. K. Langley, J. P. S. Walsh, K. S. Murray, G. Rajaraman and M. Shanmugam, *Chem. Commun.*, 2015, **51**, 3739; (c) L. Smolko, J. Černák, M. Dušek, J. Miklovič, J. Titiš and R. Boča, *Dalton Trans.*, 2015, **44**, 17565; (d) L. Smolko, J. Černák, M. Dušek, J. Titiš and R. Boča, *New J. Chem.*, 2016, **40**, 6593; (e) J. M. Zadrozny and J. R. Long, *J. Am. Chem. Soc.*, 2011, **133**, 20732; (f) J. M. Zadrozny, J. Telser and J. R. Long, *Polyhedron*, 2013, **64**, 209; (g) M. Sundararajan, D. Ganyushin, S. Ye and F. Neese, *Dalton Trans.*, 2009, 6021; (h) S. Vaidya, S. Tewary, S. K. Singh, S. K. Langley, K. S. Murray, Y. Lan, W. Wernsdorfer, G. Rajaraman and M. Shanmugam, *Inorg. Chem.*, 2016, **55**, 9564; (i) J. J. Chen and M. L. Du, *Physica B*, 1996, **228**, 409; (j) E. A. Suturina, D. Maganas, E. Bill, M. Atanasov and F. Neese, *Inorg. Chem.*, 2015, **54**, 9948; (k) J. Lu, I. O. Ozel, C. A. Belvin, X. Li, G. Skorupskii, L. Sun, B. K. Ofori-Okai, M. Dincă, N. Gedik and K. A. Nelson, *Chem. Sci.*, 2017, **8**, 7312.
15. (a) S. F. Ye and F. Neese, *J. Chem. Theory Comput.*, 2012, **8**, 2344; (b) P. J. Desrochers, J. Telser, S. A. Zvyagin, A. Ozarowski, J. Krzystek and D. A. Vicic, *Inorg. Chem.*, 2006, **45**, 8930; (c) T. Goswami and A. Misra, *J. Phys. Chem. A*, 2012, **116**, 5207; (d) J. J. Chen and M. L. Du, *Physica B*, 1996, **228**, 409; (e) H. I. Karunadasa, K. D. Arquero, L. A. Berben and J. R. Long, *Inorg. Chem.*, 2010, **49**, 4738.
16. S. Alvarez, P. Alemany, D. Casanova, J. Cirera, M. Llunell and D. Avnir, *Coord. Chem. Rev.*, 2005, **249**, 1693.
17. F. E. Mabbs and D. J. Machin, *Magnetism and Transition Metal Complexes*; Dover Publications: Mineola, NY, 2008.
18. N. F. Chilton, R. P. Anderson, L. D. Turner, A. Soncini and K. S. Murray, *J. Comput. Chem.*, 2013, **34**, 1164.
19. D. Gatteschi, R. Sessoli and J. Villain, *Molecular Nanomagnets*; Oxford University Press: Oxford, U.K. 2006.
20. (a) K. S. Cole and R. H. Cole, *J. Chem. Phys.*, 1941, **9**, 341; (b) Y.-N. Guo, G.-F. Xu, Y. Guo and J. Tang, *Dalton Trans.*, 2011, **40**, 9953.
21. (a) S. Xue, Y. N. Guo, L. Zhao, P. Zhang and J. Tang, *Dalton Trans.*, 2014, **43**, 1564; (b) P. H. Lin, T. J. Burchell, R. Clérac and M. Murugesu, *Angew. Chem., Int. Ed.*, 2008, **47**, 8848; (c) G. F. Xu, Q. L. Wang, P. Gamez, Y. Ma, R. Clérac, J. Tang, S. P. Yan, P. Cheng and D. Z. Liao, *Chem. Commun.*, 2010, **46**, 1506; (d) M. T. Gamer, Y. Lan, P. W. Roesky, A. K. Powell and R. Clérac, *Inorg. Chem.*, 2008, **47**, 6581; (e) S.-Y. Lin, C. Wang, L. Zhao and J. Tang, *Chem. Asian J.*, 2014, **9**, 3558; (f) S.-Y. Lin, L. Zhao, Y.-N. Guo, P. Zhang, Y. Guo and J. Tang, *Inorg. Chem.*, 2012, **51**, 10522; (g) R. J. Blagg, L. Ungur, F. Tuna, J. Speak, P. Comar, D. Collison, W. Wernsdorfer, E. J. L. McInnes, L. F. Chibotaru and R. E. P. Winpenny, *Nat. Chem.*, 2013, **5**, 673; (h) R. J. Blagg, F. Tuna, E. J. L. McInnes and R. E. P. Winpenny, *Chem. Commun.*, 2011, **47**, 10587; (i) K. Qian, X.-C. Huang, C. Zhou, X.-Z. You, X.-Y. Wang and K. R. Dunbar, *J. Am. Chem. Soc.*, 2013, **135**, 13302; (j) V. E. Campbell, R. Guillot, E. Rivière, P.-T. Brun, W. Wernsdorfer and T. Mallah, *Inorg. Chem.*, 2013, **52**, 5194; (k) P.-H. Lin, W.-B. Sun, M.-F. Yu, G.-M. Li, P.-F. Yan and M. Murugesu, *Chem. Commun.*, 2011, **47**, 10993; (l) G. J. Chen, C. Y. Gao, J. L. Tian, J. Tang, W. Gu, X. Liu, S. P. Yan, D. Z. Liao and P. Cheng, *Dalton Trans.*, 2011, **40**, 5579; (m) J. Long, F. Habib, P. H. Lin, I. Korobkov, G. Enright, L. Ungur, W. Wernsdorfer, L. F. Chibotaru and M. Murugesu, *J. Am. Chem. Soc.*, 2011, **133**, 5319; (n) Y.-Z. Zheng, Y. Lan, C. E. Anson and A. K. Powell, *Inorg. Chem.*, 2008, **47**, 10813; (o) J. Tang, I. Hewitt, N. T. Madhu, G. Chastanet, W. Wernsdorfer, C. E. Anson, C. Benelli, R. Sessoli and A. K. Powell, *Angew. Chem., Int. Ed.*, 2006, **45**, 1729; (p) F. Shao, B. Cahier, N. Guihéry, E. Rivière, R. Guillot, A.-L. Barra, Y. Lan, W. Wernsdorfer, V. E. Campbell and T. Mallah, *Chem. Commun.*, 2015, **51**, 16475.
22. (a) C.-S. Liu, M. Du, E. Carolina Sañudo, J. Echevarría, M. Hu, Q. Zhang, L.-M. Zhou and S.-M. Fang, *Dalton Trans.*, 2011, **40**, 9366; (b) E. Colacio, J. Ruiz-Sánchez, F. J. White and E. K. Brechin, *Inorg. Chem.*, 2011, **50**, 7268.
23. O. Kahn, *Molecular Magnetism*, VCH Publishers Inc. 1991.
24. G. M. Sheldrick, *SHELXTL Program for the Solution of Crystal of Structures*, University of Göttingen, Göttingen, Germany, 1993.
25. G. M. Sheldrick, *SHELXL 97, Program for Crystal Structure Refinement*, University of Göttingen, Göttingen, Germany, 1997.
26. A. L. Spek, *J Appl. Crystallogr.*, 2003, **36**, 7.
27. L. J. Farrugia, *J. Appl. Crystallogr.*, 1999, **32**, 837.
28. (a) K. M. Lancaster, M.-E. Zaballa, S. Sproules, M. Sundararajan, S. DeBeer, J. H. Richards, A. J. Vila, F. Neese and H. B. Gray, *J. Am. Chem. Soc.*, 2012, **134**, 8241; (b) M. Sundararajan and F. Neese, *Inorg. Chem.*, 2015, **54**, 7209; (c) B. Sadhu, M. Sundararajan and T. Bandyopadhyay, *Inorg. Chem.*, 2016, **55**, 598; (d) B. Sadhu and M. Sundararajan, *Phys. Chem. Chem. Phys.*, 2016, **18**, 16748.
29. (a) F. Neese, *WIREs Comput. Mol. Sci.*, 2012, **2**, 73; (b) F. Neese, *Wiley Interdiscip. Rev. Comput. Mol. Sci.*, 2017, **8**, 1; (c) T. Noro, M. Sekiya and T. Koga, *Theoret. Chem. Acc.*, 2012, **131**, 1124.
30. D. Ganyushin and F. Neese, *J. Chem. Phys.*, 2008, **128**, 114117.

Table of Contents



The influence of ligand field strength on magnetic anisotropy of a series of isostructural tetrahedral Co^{II} complexes has been investigated by using a combined experimental and theoretical approach.